Biochemical and Biophysical Research Communications 495 (2018) 1264–1270

Contents lists available at ScienceDirect

Biochemical and Biophysical Research Communications

journal homepage: www.elsevier.com/locate/ybbrc

Human adipose-derived stem cells and simvastatin-functionalized biomimetic calcium phosphate to construct a novel tissue-engineered bone

Xiao Zhang [a, b, 1], Weiran Jiang [a, b, 1], Yunsong Liu [a, b], Ping Zhang [a, b], Linchuan Wang [a, b], Wenyue Li [a, b], Gang Wu [c, *], Yanjun Ge [a, b, **], Yongsheng Zhou [a, b]

[a] Department of Prosthodontics, Peking University School and Hospital of Stomatology, Beijing, 100081, China
[b] National Engineering Lab for Digital and Material Technology of Stomatology, Beijing Key Laboratory of Digital Stomatology, Peking University School and Hospital of Stomatology, Beijing, 100081, China
[c] Department of Oral Implantology and Prosthetic Dentistry, Academic Centre for Dentistry Amsterdam (ACTA), Universiteit van Amsterdam and Vrije Universiteit Amsterdam, Amsterdam, The Netherlands

ARTICLE INFO

Article history:
Received 11 November 2017
Accepted 17 November 2017
Available online 24 November 2017

Keywords:
Human adipose-derived stem cells
Simvastatin
Biomimetic
Calcium phosphate
Tissue-engineered bone

ABSTRACT

To repair bone defects, we evaluate the *in-vitro* and *in-vivo* osteogenic activities of a novel tissue-engineered bone (TEB) by elaborately combining biomimetic calcium phosphate (BioCaP) granules with internally-incorporated simvastatin (SIM) and human adipose-derived stem cells (hASCs). First, we constructed BioCaP with SIM internally incorporated (SIM-BioCaP). Then we characterized the morphology and chemical composition of SIM-BioCaP. The release kinetics of SIM was monitored *in vitro* spectroscopically. Thereafter, we explored the *in-vitro* cellular responses of hASCs to SIM-BioCaP by performing scanning electron microscopy observation, proliferation assay, alkaline phosphatase (ALP) activity assay, alizarin red staining and real-time PCR. Finally, we investigated the *in-vivo* osteogenic activities of the novel TEB in a subcutaneous bone induction model in nude mice. We found that SIM was successfully incorporated internally in BioCaP and showed a slow release manner without significantly affecting the attachment and proliferation of hASCs. The released SIM from BioCaP could significantly enhance the proliferation, ALP activities, mineralized nodules formation and osteogenic genes of hASCs. The *in-vivo* tests showed this TEB could induce new bone formation while the other groups could not. Taken together, the present data show that this novel TEB represented a very promising construct to treat critical-volume bone defects.

1. Introduction

Critical-sized bone defects, resulting from congenital nonunion, trauma, inflammation, and osteosarcoma resection, can severely compromise aesthetics and musculoskeletal functions [1]. In the clinic, the application of autografts is limited because of the low available quantity as well as donor-site pain and morbidity [2]. Consequently, various alternative biomaterials are being developed to facilitate osseous restoration in the clinic.

Synthetic CaP-based materials are widely adopted, due to their good biocompatibility, biodegradability, and osteoconductivity [3–7]. However, they are still too limited to realize osseous restoration because of the intrinsically lack of osteoinductivity. One promising approach to this problem is to confer osteoinductivity to these CaP-based materials by using an osteoinductive agent. We

Abbreviations: TEB, tissue-engineered bone; BioCaP, biomimetic calcium phosphate; SIM, simvastatin; hASCs, human adipose-derived stem cells; SEM, scanning electron microscopy; ALP, alkaline phosphatase; BMP-2, bone morphogenetic protein-2; BMSCs, bone marrow-derived stem cells; PBS, phosphate buffered solution; ECM, extracellular matrix; HE, hematoxylin and eosin; PM, proliferation medium; OM, osteogenic medium; CCK-8, cell-counting kit-8; *Runx2*, *runt related transcription factor 2*; *ALP*, *alkaline phosphatase*; *OSX*, *osterix*; *OC*, *osteocalcin*; CaP, calcium phosphate; EDS, energy dispersive X-ray spectroscopy; PM, proliferation medium; OM, osteogenic medium.

* Corresponding author. Gustav mahlerlaan 3004, 1081 LA Amsterdam, The Netherlands.
** Corresponding author. Zhongguancun South Avenue 22, Haidian District, Beijing 100081, China.
E-mail addresses: g.wu@acta.nl (G. Wu), yanjun_ge@163.com (Y. Ge).
[1] These authors contributed equally to this work.

https://doi.org/10.1016/j.bbrc.2017.11.150
0006-291X/

and other researchers have confirmed that simvastatin (SIM) could increase the *in-vitro* osteogenic capability and promote the *in-vivo* bone formation of human adipose-derived stem cells (hASCs) and bone marrow-derived stem cells (BMSCs) [8,9]. Since it is also stable, inexpensive and available in large quantity, SIM shows a very promising application potential for bone tissue engineering. However, if the dose of SIM is much higher than the requirement for bone formation, this may potentially cause a series of side effects, such as myotoxicity, liver failure and kidney failure [10]. In order to exert the optimal efficacy, a local release system is preferred to deliver SIM to targeted sites. Furthermore, SIM needs to be delivered in a slow and sustained release profile, instead of in a single high-dose burst [11].

By delicately developing the biomimetic technique, we recently constructed a novel millimeter-scale CaP granules named biomimetic calcium phosphate (BioCaP) [12], which maintain the biomimetic property so that they can internally incorporate bioactive reagents and realize their slow and local release throughout the degradation process. We showed that the slowly and locally released bone morphogenetic protein-2 (BMP-2) that were internally incorporated into the BioCaP could induce ectopic bone formation [12]. However, the vulnerability to sterilization, high price, and limited availability largely constrain the application potential of BMP-2. In contrast, SIM is much more stable and less expensive, which makes SIM more feasible and promising for clinical translation.

In this study, we wished to develop a novel tissue engineered bone (TEB) by elaborately combining BioCaP with internally-incorporated SIM and hASCs. We assessed the physicochemical properties of, the *in-vitro* cellular responses to, and the *in-vivo* osteogenic activity of the novel TEB.

2. Materials and methods

2.1. Fabrication of biomimetic calcium phosphate (BioCaP) and SIM incorporation

In this study, BioCaP were produced according to previously reported procedures [12]. Briefly, a supersaturated CaP solution, buffered to pH 7.4 with 250 mM Tris, was incubated in a shaking water bath at 37 °C. SIM (10 μM) was added to this CaP solution and co-precipitated into the interior of BioCaP. After 24h of incubation, the precipitation was retrieved, gently washed by phosphate-buffered saline (PBS), filtered using a vacuum exhaust filtering method with a vacuum filter (0.22 μm pore, Corning, NY, USA) and an air pump. All the procedures were performed under aseptic conditions.

2.2. Characteristics of the SIM-BioCaP surfaces

Field emission scanning electron microscopy (SEM) (FESEM, S-4800; HITACHI, Japan) and energy dispersive X-ray spectroscopy (EDS) were used to analyze the morphology and elementary components of the surface of SIM-BioCaP. BioCaP in the absence of SIM was used as control.

2.3. Release kinetics of SIM-BioCaP

According to our previous experiments [13], BioCaP loaded with SIM (10 μM) were immersed in 200 μL PBS using a 48-well plate. BioCaP in the absence of SIM was used as control. All plates were kept at 37 °C with shaking at a rate of 60 rpm. At predetermined time intervals of 1, 2, 3, 4, 5, 6, 7, 10, 14, and 21 days, the SIM contents were measured using a Multimode Plate Reader (EnSpire, PerkinElmer Co., Shelton, CT, USA) at a wavelength of 238 nm.

2.4. Cell culture

hASCs of three different healthy donors were purchased from ScienCell Company (7510, ScienCell, San Diego, CA, USA). All cell-based experiments were repeated at least three times.

2.5. Proliferation and osteogenic differentiation of hASCs stimulated by SIM-BioCaP

Experimental design. Third passage cells were used for the following experiments, and all experiments using hASCs from the three donors. BioCaP and SIM-BioCaP were immersed in proliferation medium (PM) or osteogenic medium (OM) respectively. The supernatants were collected every two days and used to culture hASCs. The hASCs were exposed to four different supernatants derived from (i) PM + BioCaP, (ii) PM + SIM-BioCaP, (iii) OM + BioCaP, or (iv) OM + SIM-BioCaP, respectively.

Cell attachment assay. The hASCs were seeded onto sterilized BioCaP or SIM-BioCaP respectively. After 2 h and 24 h, the constructs were rinsed by PBS and fixed overnight in cacodylate buffered 4% glutaraldehyde at 4 °C. The specimens were postfixed in 1% OsO_4 for 1.5 h, dehydrated with a graded series of ethanol, dried in a critical point dryer (Micro Modul YO-230, Thermo Scientific, Waltham, MA, USA), mounted onto aluminum stubs, sputter coated with gold, and viewed under a field emission SEM, as described previously [13].

Cell proliferation assay. The hASCs were seeded in 12-well plates and cultured with PM or PM + released SIM, respectively. To investigate their proliferation in response to SIM, cell numbers were determined using the CCK-8 according to the manufacturer's instructions (Dojindo Laboratories, Kumamoto, Japan). Growth curves were drawn according to the absorbance values.

Cell differentiation assay. The hASCs were seeded in 12-well plates and divided into four groups as above. ALP staining was performed on days 4 and 7 as described in detail previously [14]. ALP activity was determined using an ALP kit according to the manufacturer's protocol, and normalized to total protein content. To assess mineralization, hASCs were seeded in 12-well plates and cultured with OM or OM + released SIM, respectively. Alizarin red staining and mineralization assays were performed as described previously on days 14 [15].

Real-time quantitative PCR analysis. The hASCs were seeded in 6-well plates and divided into four groups as above. After 4 and 7 days osteoinduction, total RNA was isolated according to the manufacturer's protocol (Invitrogen, Carlsbad, CA, USA) and two microgram aliquots of RNA were reverse-transcribed according to the manufacturer's instruction (Roche, Basel, Switzerland). Real-time quantitative PCR assays were performed by using a Power SYBR Green PCR Master Mix and an ABI PRISM 7500 sequence detection system (Applied Biosystems, Foster City, CA, USA). The primers for *Runt related transcription factor 2* (*RUNX2*), *ALP*, *osterix (OSX)*, and *osteocalcin (OC)* were synthesized by Invitrogen and are listed in Supplementary Table 1. *Glyceraldehyde 3-phosphate dehydrogenase* (*GAPDH*) was used as an internal standard [15].

Animal experiments. Four groups were used to conduct the *in vivo* study: (a) BioCaP only; (b) BioCaP + hASCs; (c) SIM-BioCaP; (d) SIM-BioCaP + hASCs. The nude mice were anaesthetized firstly and four respective enclosed transplantation sites were prepared by means of hemostatic forceps in the dorsal subcutaneous space. Subsequently, the four groups of BioCaP complexes were implanted aseptically into the four different sites ($n = 5$ per group). Each group contained 40 mg BioCaP granules [15]. As the results of EDS showed the weight percentage of SIM in SIM-BioCaP was 5.13%, so each SIM-BioCaP granules sample contained 40 mg × 5.13 % ≈ 2.05 mg SIM.

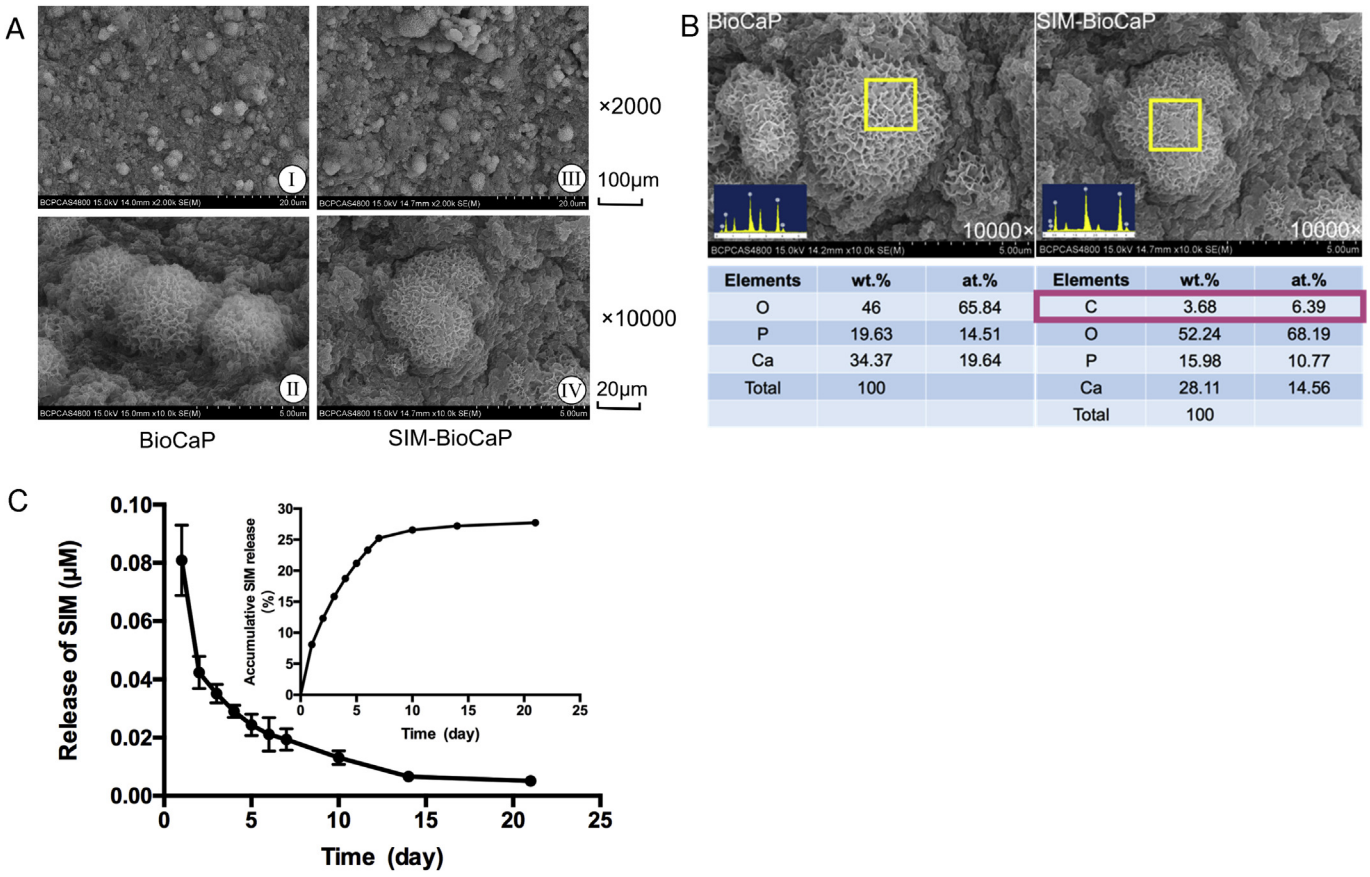

Elements	wt.%	at.%
O	46	65.84
P	19.63	14.51
Ca	34.37	19.64
Total	100	

Elements	wt.%	at.%
C	3.68	6.39
O	52.24	68.19
P	15.98	10.77
Ca	28.11	14.56
Total	100	

Fig. 1. *In-vitro* characterization of physicochemical properties of SIM-BioCaP and release kinetics of SIM from SIM-BioCaP. (A) The morphology of BioCaP (I, II). The morphology of SIM-BioCaP (III, IV). (B) The composition of BioCaP and SIM-BioCaP. (C) The release kinetics of SIM from SIM-BioCaP. BioCaP, biomimetic calcium phosphate; SIM, simvastatin.

Analyses of bone formation. As described in our previous study [15], specimens of each group were harvested at 4 weeks after *in vivo* implantation, and animals in each group were sacrificed by CO_2 asphyxiation. Soft X-ray examinations were used to evaluate the mineral density and the relative gray-scale was determined by Image J software (National Institutes of Health, USA). The bone constructs were fixed in 4% paraformaldehyde and then decalcified for 10 days in 10% EDTA (pH 7.4). Following decalcification, the specimens were dehydrated and subsequently embedded in paraffin. Sections (5 μm thickness) were stained with HE.

2.6. Statistical analysis

Data were analyzed using SPSS software (Chicago, IL, USA). Statistical analysis of the data was performed by one-way analysis of variance (ANOVA), and post hoc test for multiple comparisons was carried out using the Fisher LSD test. When variance was not homogeneous, the Kruskal-Wallis test was used, followed by the Nemenyi test for multiple comparisons. For all tests, statistical significances were accepted for *P*-values lower than 0.05.

The details of materials and methods can be found at supplementary materials.

3. Results

3.1. In-vitro characterization of physicochemical properties of SIM-BioCaP

The result of SEM showed that the BioCaP was composed of rough matrix containing tiny crystals and spherical globules containing bent lamina-like crystals. The size of the crystal units varied approximately from 5 to 10 μm (Fig. 1A I, II). The internally-incorporation of SIM didn't significantly influence the morphology of BioCaP (Fig. 1A III, IV). EDS analysis of the elementary components showed that the BioCaP was mainly composed of the elements calcium, phosphate and oxygen (left panel in Fig. 1B). On SIM-BioCaP, carbon (C) was detected (right panel in Fig. 1B), which confirmed that SIM was successfully incorporated internally into the BioCaP scaffold. The details of the results can be found at supplementary materials.

3.2. Release kinetics of SIM from SIM-loaded BioCaP

The release curve of SIM showed a triphasic pattern: an initial 1-day burst release, an intermediate-speed release from 2 to 7 days and a slow release from 8 days. In the 1st day, 8.08% was released. In the end of the medium release phase, 25.2% of SIM was released with an average rate of 2.86% per day. In the slow release period (from day 8), the release rate maintained at approximately 0.18% per day, and the concentration of SIM in the culture well remained at 0.01 μM (Fig. 1C).

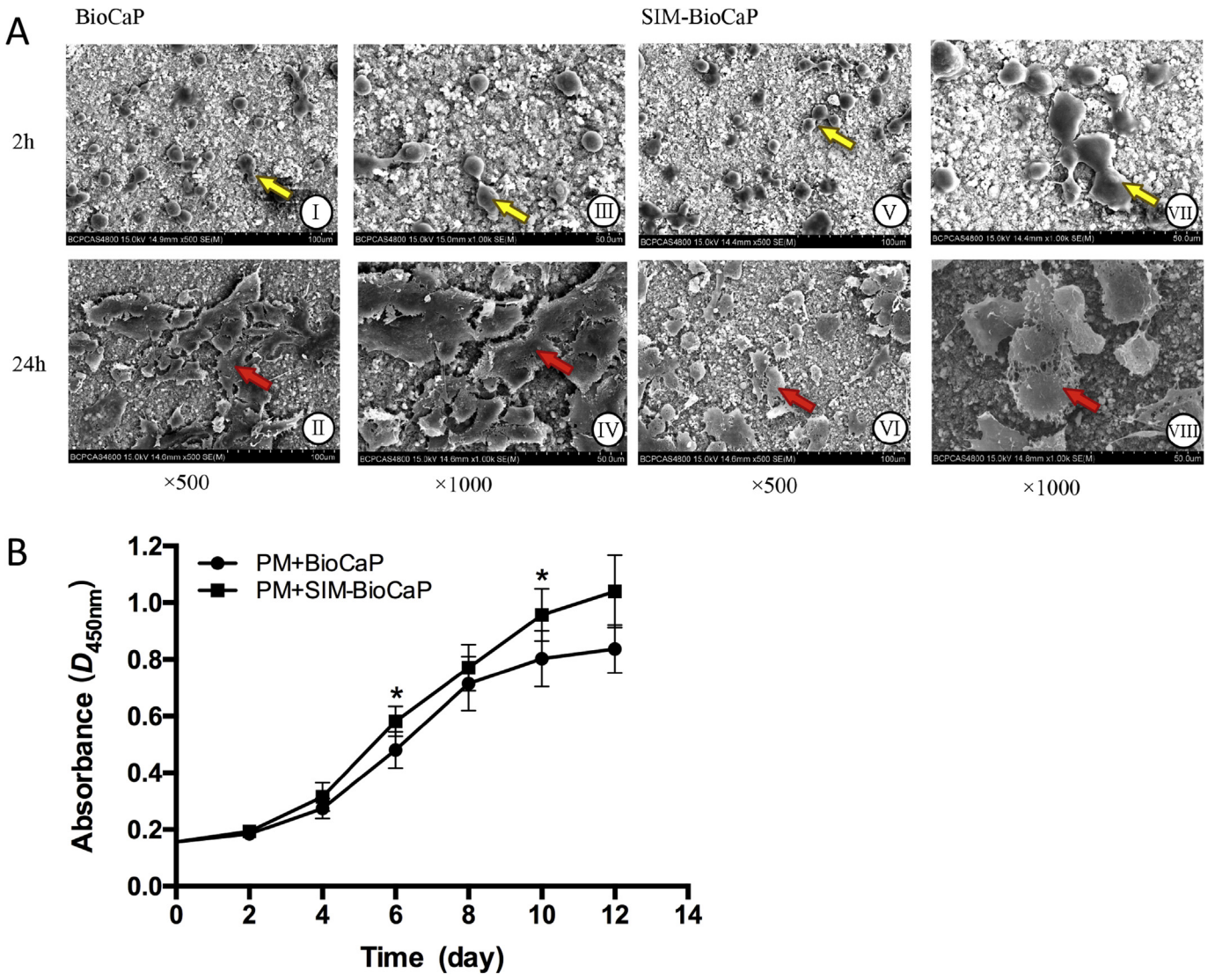

Fig. 2. Effect of SIM-BioCaP on cell attachment and proliferation. (A) The attachment of hASCs on SIM-BioCaP after culturing for 2 h (I, III, V, VII) and 24 h (II, IV, VI, VIII). Yellow arrows point to hASCs. Red arrows point to extracellular matrix. (B) The results of CCK-8. hASCs, human adipose-derived stem cells; BioCaP, biomimetic calcium phosphate; SIM, simvastatin; PM, proliferation medium. *$P < 0.05$ compared to PM. (For interpretation of the references to colour in this figure legend, the reader is referred to the web version of this article.)

3.3. In-vitro cellular response of hASCs to SIM-BioCaP

3.3.1. Effect of SIM-BioCaP on cell attachment and proliferation

The hASCs were able to attach to the surface of BioCaP and SIM-BioCaP (Fig. 2A). 2 h post seeding, cells have already extended obvious lamellipodia on the surfaces of both BioCaP and SIM-BioCaP. At 24 h, the cells have also shown a full-spreading status with a larger polygonal morphology (Fig. 2A). As the result of CCK-8 showed, on the 6th and 10th day, the supernatant collected from PM + SIM-BioCaP could result in significantly higher cell proliferation than that from the PM + BioCaP (Fig. 2B).

3.3.2. Effects of SIM-BioCaP on the osteogenic differentiation of hASCs

SIM was unable to promote ALP activity in the presence of PM after a 4-day induction. However, after 7 days of induction, PM + SIM-BioCaP could significantly enhance ALP activity when compared with PM + BioCaP ($P < 0.05$). 4 and 7 days post induction, OM + SIM-BioCaP significantly increased the ALP activity and staining of hASCs when compared with other groups ($P < 0.05$) (Fig. 3A and B).

Alizarin red staining and quantification assays demonstrated that hASCs cell matrix calcifications were significantly elevated 2.8 folds after a 14-day induction by in the OM + SIM-BioCaP group, compared to the OM + BioCaP ($P < 0.05$) (Fig. 3C and D).

7 days post induction, the expression of osteogenic genes (*RUNX2, ALP, OSX, OC*) were significantly up-regulated in OM + SIM-BioCaP, compared to other groups ($P < 0.05$). Moreover, the expression levels were continually elevated from day 7–14 (Fig. 3E, F, G, H).

3.4. In-vivo bone formation capability of SIM-BioCaP

Four weeks post implantation, soft X-ray examination showed that group (d) could form bone-like tissues with a relatively higher density than other groups (Fig. 4A). In grey-scale assessment, the grey-scales in the group of (c) and (d) were significantly higher than other two groups without SIM ($P < 0.05$) (Fig. 4B). Moreover, the greay-scale of (d) group was the highest (Fig. 4B).

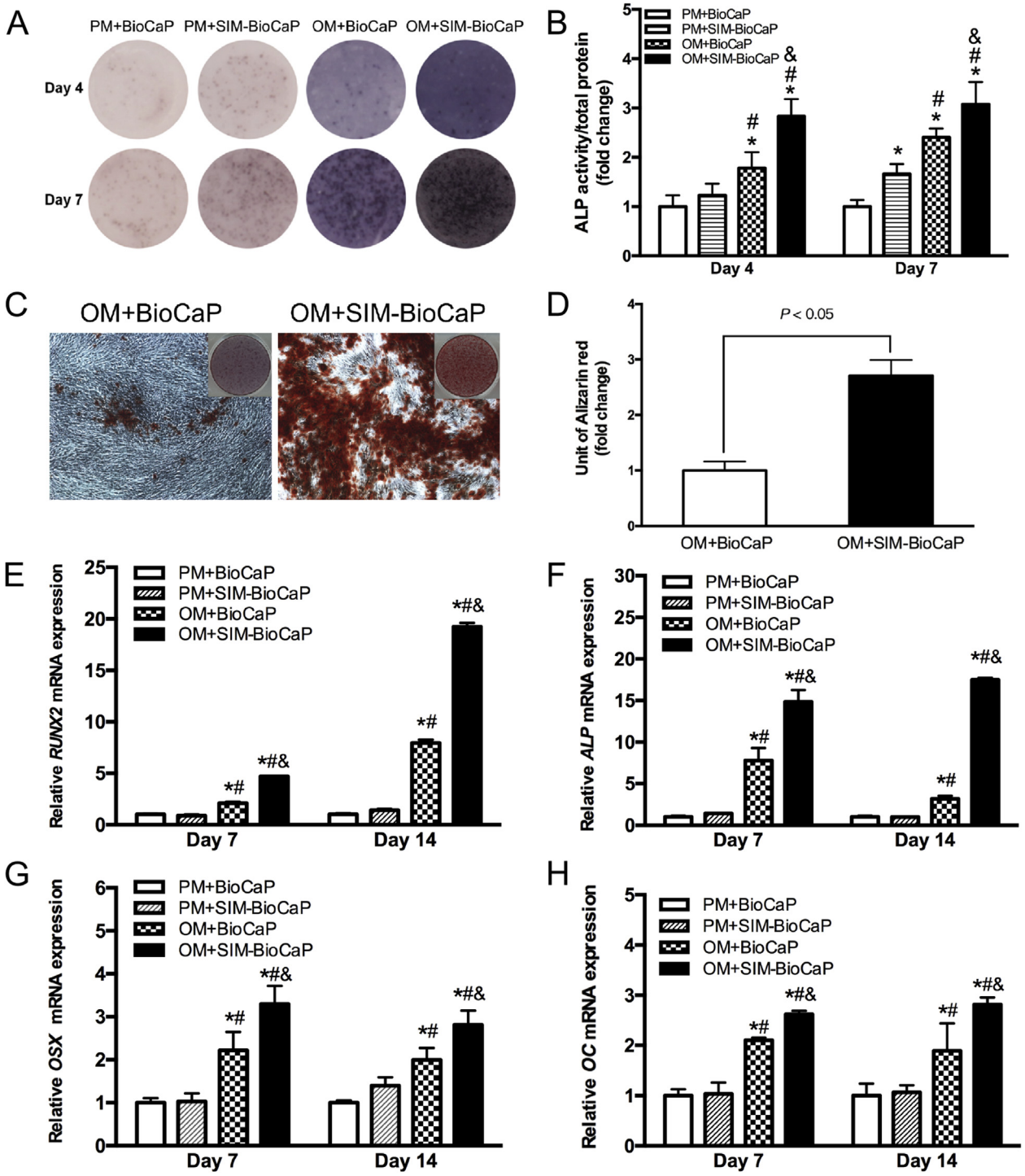

Fig. 3. Effects of SIM-BioCaP on the osteogenic differentiation of hASCs. (A) The results of ALP staning after 4 and 7 days induction. (B) The results of ALP activities after 4 and 7 days induction. (C) Alizarin red staining result after 14 days induction. (D) Mineralization assays results after 14 days induction. (E,F,G,H) Osteogenesis-associated gene (*RUNX2, ALP, OSX, OC*) expressions of hASCs induced after 7 days and 14 days. BioCaP, biomimetic calcium phosphate; SIM, simvastatin; PM, proliferation medium; OM, osteogenic medium. ALP, alkaline phosphatase. *Runx2, runt related transcription factor 2*; *ALP, alkaline phosphatase*; *OSX, osterix*; *OC, osteocalcin*; hASCs, human adipose-derived stem cells $^{*}P < 0.05$ compared to PM + BioCaP; $^{\#}P < 0.05$ compared to PM + SIM-BioCaP; $^{\&}P < 0.05$ compared to OM + BioCaP. (For interpretation of the references to colour in this figure legend, the reader is referred to the web version of this article.)

The results of HE staining showed that, in the group (d), the eosinophilic bone-like tissues could be found in the ECM around the scaffold materials (Fig. 4C d), whereas there was no typical bone-like structure in the ECM in other three groups (Fig. 4C a, b, c).

4. Discussion

Bone tissue engineering is an interdisciplinary technology that elaborately combines the knowledges and technologies in material engineering, cell technology and bioactive reagents with a final goal to regenerate bone tissues in large defects [16]. In this study, we, for the first time, successfully constructed a TEB by elaborately combining BioCaP with internally-incorporated SIM and hASCs. Our data showed that the slowly-released SIM from BioCaP could retain its bioactivity and significantly enhance the *in-vitro* osteogenic differentiation of hASCs. Furthermore, this TEB could generate new bone formation even in a subcutaneous pro-fibrotic site, which indicated the its osteoinductive property. Consequently, the novel TEB of SIM-BioCaP/hASCs showed a very promising application potential to treat critical-volume bone defects.

The positive interaction among materials, cells and bioactive reagents is highly critical for the success of bone tissue engineering [17]. The application of hASCs in bone tissue engineering is highly attractive due to their easier accessibility, lower donor site morbidity and larger availability than other mesenchymal stem cells [18,19]. However, hASCs can be, to some extent, committed to adipogenic differentiation [1]. In comparison with the dual stimulating effects of BMPs on adipogenic and osteogenic differentiation, SIM can suppress the adipogenic differentiation and enhance the osteogenic differentiation of mesenchymal stem cells [20]. Consequently, SIM may be more suitable to favor hASCs-based tissue engineering technique than BMP-2. SIM can enhance the *in-vitro* and *in-vivo* osteogenesis of hASCs by significantly increasing the expression of mRNA encoding *BMP-2, Runx2, VEGF* and *FGF-2*, among which the promoting effect of simvastatin seems to be largely attributed to its induced endogenous *BMP-2* [8]. This phenomenon highly suggested that the suppressive effect of SIM on the adipogenic differentiation of hASCs was critical to favor the osteogenic differentiation of hASCs.

On the other hand, SIM needs to be delivered to the targeted sites in a slow and sustained release profile, instead of in a single high-dose burst to achieve a maximal efficacy [11]. Therefore, a proper scaffold is highly important. One of the most widely used biomaterials for bone regeneration is CaP. However, most of the CaP materials is processed by sintering synthetic or naturally-derived. Therefore, bioactive reagents can only be superficially adsorbed onto the materials, which is associated with a burst release profile of these bioactive agents. Furthermore, these sintered materials show a low biodegradability, which hinder the complete substitution with natural bone tissue. By following the biomimetic principle, we recently made successfully develop novel CaP millimeter-scale granules – BioCaP [12] without sintering. Thanks to the biomimetic production procedure, BioCaP showed a natural cancellous bone-like stiffness and gained a “smart” biodegradability: the more the new bone formed, the faster the material the material degraded [12]. The most invaluable property of BioCaP is that it maintains the biomimetic property so that they can internally incorporate bioactive reagents and realize their slow and local release throughout the degradation process [12]. Even the vulnerable proteinous osteoinductive agents (e.g. BMP-2) can be easily internally incorporated into BioCaP and retain its bioactivity [12]. With all these exciting findings, we believe that BioCaP can serve as a suitable carrier of SIM for hASCs-based tissue engineering. Consequently, in this study, we elaborately constructed the TEB by combining the BioCaP with internally incorporated SIM and hASCs.

We showed that SIM could be successfully incorporated internally into the BioCaP with a weight percentage of about 5.13%. The incorporation of SIM into BioCaP affect neither the topography of BioCaP (Fig. 1A) nor the attachment of hASCs (Fig. 2A). Furthermore, the released SIM from BioCaP could promote the proliferation of hASCs more effectively compared to control medium (Fig. 2B). When loaded into other slow-delivery systems, SIM could be released in a sustained manner, and the cumulative rate reached between 70 % and 100% at the end of 21 days [7,21–23]. Similarly, in our previous study, we demonstrated the controlled release of SIM from biomimetic CaP coating was almost completed in 21 days [13]. In contrast, in this study, the cumulative rate of SIM released was only 27.7% by 21 days, which indicated that the release rate of the internally-incorporated SIM from BioCaP was markedly lower than other systems. This characteristic release profile makes the SIM-BioCaP a superior system for hASCs-based bone tissue engineering. During the release kinetic phase, after the preliminiary

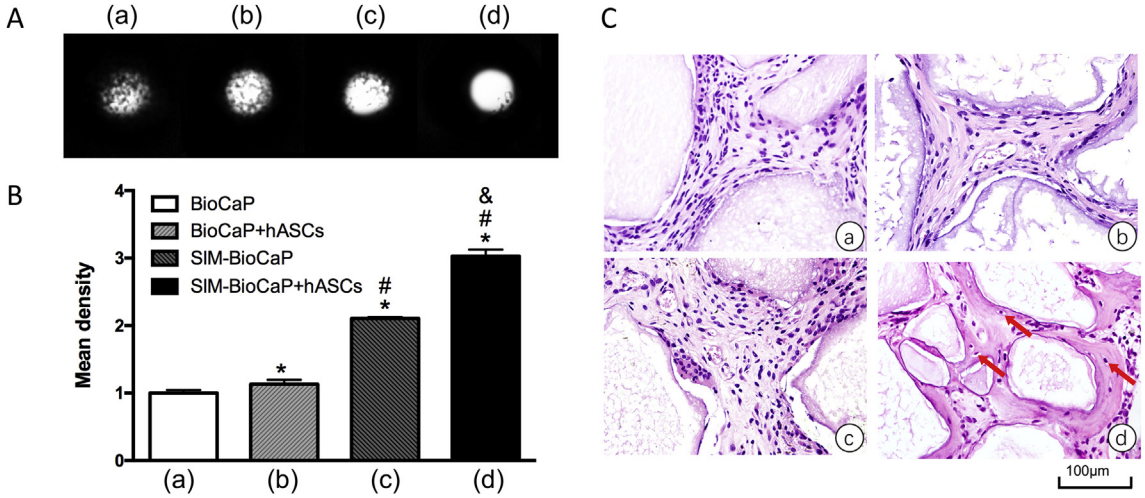

Fig. 4. Soft X-ray examination and histological analyses of SIM + BioCaP + hASC complex implanted into nude mice for 4 weeks. (A) The soft X-ray radiography results. (B) Relative grey scales were determined by Image J software. (C) HE staining results. (a) BioCaP; (b) BioCaP + hASCs; (c) SIM-BioCaP; (d) SIM-BioCaP + hASCs. Red arrows point to osteocytes. $^{*}P < 0.05$ compared to BioCaP; $^{\#}P < 0.05$ compared to BioCaP + hASCs; $^{\&}P < 0.05$ compared to SIM-BioCaP. hASCs, human adipose-derived stem cells; BioCaP, biomimetic calcium phosphate; SIM, simvastatin. (For interpretation of the references to colour in this figure legend, the reader is referred to the web version of this article.)

experiment, we found when SIM (10 μM) was added to this CaP solution and co-precipitated into the interior of BioCaP, the concentration of SIM could remain above 0.01 μM even after 10 days (Fig. 1C). We previously demonstrated that SIM at 0.01, 0.1, and 1 μM could enhance the osteogenic differentiation of hASCs [8]. Therefore, the slow and sustained delivery of SIM from BioCaP could continuously stimulate the osteogenesis of hASCs *in vitro*. We further proved that the released SIM from BioCaP could also retain its bioactivity and induce the *in-vitro* osteogenic differentiation of hASCs. The cell differentiation experiments, including ALP staining and quantitative assay, alizarin red staining and mineralization assay, and osteogenic gene expression, confirmed the osteoinductive effect of SIM-BioCaP on hASCs (Fig. 3).

In the subsequent *in-vivo* experiments, consistent with the *in vitro* findings, SIM-BioCaP + hASCs complex could result in new bone formation even in a subcutaneous pro-fibrotic microenvironment, which substantially corroborated the osteoinductive property of this novel TEB (Fig. 4). In contrast, no bone formation was detected in the other groups which indicated that the combination of SIM and hASCs was of paramount importance for new bone formation (Fig. 4C). These positive results also indicated that an *in-vitro* pre-induction of hASCs was not a requirement for its *in-vivo* osteogenic activity.

Considering the large availability of hASCs, the low cost of SIM and the favourable physicochemical/biological properties BioCaP, this novel TEB represents a promising method for bone regeneration, and can be easily translated to clinical applications. Moreover, by combining surface coating, BioCaP can be further modified to form a dual release system for a sequential delivery of different drugs [12]. In our previous study, we constructed a CaP coating integrated with SIM and metronidazole, and demonstrated the multifunctional potential of this CaP coating in combination with osteoinductive and antibacterial effects [13]. Similarly, we can incorporate SIM into the interior of BioCaP, and incorporate antibacterial agents onto the surface coating. The combination of two bioactive agents does confer osteoinductivity and antibacterial capabilities on BioCaP simultaneously, which can be a new strategy for the treatment of bone defects with bacterial infections.

Conflicts of interest

The authors declare no conflict of interest.

Acknowledgements

This study was supported by grants from the National Natural Science Foundation of China [81400484], the Project for Culturing Leading Talents in Scientific and Technological Innovation of Beijing [Z171100001117169], and Youth Foundation of Peking University School and Hospital of Stomatology [YS020213].

Appendix A. Supplementary data

Supplementary data related to this article can be found at https://doi.org/10.1016/j.bbrc.2017.11.150.

Transparency document

Transparency document related to this article can be found online at https://doi.org/10.1016/j.bbrc.2017.11.150.

References

[1] X. Zhang, J. Guo, Y. Zhou, G. Wu, The roles of bone morphogenetic proteins and their signaling in the osteogenesis of adipose-derived stem cells, Tissue Eng. Part B Rev. 20 (2014) 84–92.
[2] Y. Zheng, G. Wu, T. Liu, Y. Liu, D. Wismeijer, Y. Liu, A novel bmp2-coprecipitated, layer-by-layer assembled biomimetic calcium phosphate particle: a biodegradable and highly efficient osteoinducer, Clin. implant Dent. Relat. Res. (2013) 645–654.
[3] E. Verron, I. Khairoun, J. Guicheux, J.M. Bouler, Calcium phosphate biomaterials as bone drug delivery systems: a review, Drug Discov. Today 15 (2010) 547–552.
[4] S.V. Dorozhkin, Bioceramics of calcium orthophosphates, Biomaterials 31 (2010) 1465–1485.
[5] P. Wang, L. Zhao, W. Chen, X. Liu, M.D. Weir, H.H. Xu, Stem cells and calcium phosphate cement scaffolds for bone regeneration, J. Dent. Res. 93 (2014) 618–625.
[6] R. Agarwal, A.J. Garcia, Biomaterial strategies for engineering implants for enhanced osseointegration and bone repair, Adv. Drug Deliv. Rev. 94 (2015) 53–62.
[7] H.X. Zhang, G.Y. Xiao, X. Wang, Z.G. Dong, Z.Y. Ma, L. Li, Y.H. Li, X. Pan, L. Nie, Biocompatibility and osteogenesis of calcium phosphate composite scaffolds containing simvastatin-loaded plga microspheres for bone tissue engineering, J. Biomed. Mater Res. A 103 (2015) 3250–3258.
[8] Y. Zhou, Y. Ni, Y. Liu, B. Zeng, Y. Xu, W. Ge, The role of simvastatin in the osteogenesis of injectable tissue-engineered bone based on human adipose-derived stromal cells and platelet-rich plasma, Biomaterials 31 (2010) 5325–5335.
[9] Y.S. Liu, M.E. Ou, H. Liu, M. Gu, L.W. Lv, C. Fan, T. Chen, X.H. Zhao, C.Y. Jin, X. Zhang, et al., The effect of simvastatin on chemotactic capability of sdf-1alpha and the promotion of bone regeneration, Biomaterials 35 (2014) 4489–4498.
[10] A. Oryan, A. Kamali, A. Moshiri, Potential mechanisms and applications of statins on osteogenesis: current modalities, conflicts and future directions, J. Control Release 215 (2015) 12–24.
[11] Y.C. Fu, Y.H. Wang, C.H. Chen, C.K. Wang, G.J. Wang, M.L. Ho, Combination of calcium sulfate and simvastatin-controlled release microspheres enhances bone repair in critical-sized rat calvarial bone defects, Int. J. Nanomedicine 10 (2015) 7231–7240.
[12] T. Liu, G. Wu, Y. Zheng, D. Wismeijer, V. Everts, Y. Liu, Cell-mediated bmp-2 release from a novel dual-drug delivery system promotes bone formation, Clin. Oral Implants Res. 25 (2014) 1412–1421.
[13] Y. Liu, X. Zhang, X. Jin, C. Fan, H. Ye, M. Ou, L. Lv, G. Wu, Y. Zhou, Bi-functionalization of a calcium phosphate-coated titanium surface with slow-release simvastatin and metronidazole to provide antibacterial activities and pro-osteodifferentiation capabilities, PLoS One 9 (2014) e97741.
[14] Y. Liu, Y. Zhao, X. Zhang, T. Chen, X. Zhao, G.E. Ma, Y. Zhou, Flow cytometric cell sorting and in vitro pre-osteoinduction are not requirements for in vivo bone formation by human adipose-derived stromal cells, PLoS One 8 (2013) e56002.
[15] X. Zhang, J. Guo, G. Wu, Y. Zhou, Effects of heterodimeric bone morphogenetic protein-2/7 on osteogenesis of human adipose-derived stem cells, Cell Prolif. 48 (2015) 650–660.
[16] Y. Liu, G. Wu, K. de Groot, Biomimetic coatings for bone tissue engineering of critical-sized defects, J. R. Soc. Interface 7 (Suppl 5) (2010) S631–S647.
[17] G.J. Meijer, J.D. de Bruijn, R. Koole, C.A. van Blitterswijk, Cell-based bone tissue engineering, PLoS Med. 4 (2007) e9.
[18] P.A. Zuk, M. Zhu, P. Ashjian, D.A. De Ugarte, J.I. Huang, H. Mizuno, Z.C. Alfonso, J.K. Fraser, P. Benhaim, M.H. Hedrick, Human adipose tissue is a source of multipotent stem cells, Mol. Biol. cell 13 (2002) 4279–4295.
[19] P.A. Zuk, M. Zhu, H. Mizuno, J. Huang, J.W. Futrell, A.J. Katz, P. Benhaim, H.P. Lorenz, M.H. Hedrick, Multilineage cells from human adipose tissue: implications for cell-based therapies, Tissue Eng. 7 (2001) 211–228.
[20] C. Song, Z. Guo, Q. Ma, Z. Chen, Z. Liu, H. Jia, G. Dang, Simvastatin induces osteoblastic differentiation and inhibits adipocytic differentiation in mouse bone marrow stromal cells, Biochem. Biophys. Res. Commun. 308 (2003) 458–462.
[21] J. Zhang, H. Wang, J. Shi, Y. Wang, K. Lai, X. Yang, X. Chen, G. Yang, Combination of simvastatin, calcium silicate/gypsum, and gelatin and bone regeneration in rabbit calvarial defects, Sci. Rep. 6 (2016) 23422.
[22] R.;T.,S.J.K. Masaeli, R. Dinarvand, M. Tahriri, V. Rakhshan, M. Esfandyari-Manesh, Preparation, characterization and evaluation of drug release properties of simvastatin-loaded plga microspheres, Iran. J. Pharm. Res. 15 (2016) 205–211.
[23] K. Wang, Y. Wang, X. Zhao, Y. Li, T. Yang, X. Zhang, X. Wu, Sustained release of simvastatin from hollow carbonated hydroxyapatite microspheres prepared by aspartic acid and sodium dodecyl sulfate, Mater Sci. Eng. C Mater Biol. Appl. 75 (2017) 565–571.